

## ON THE CONVERSION OF PLASTIC WORK INTO HEAT DURING HIGH-STRAIN-RATE DEFORMATION

Guruswami Ravichandran<sup>1</sup>, Ares J. Rosakis<sup>1</sup>, Jon Hodowanyc<sup>2</sup> and Phoebus Rosakis<sup>3</sup>

<sup>1</sup>*Graduate Aeronautical Laboratories, California Institute of Technology, Pasadena, CA 91125*

<sup>2</sup>*Rosetta Inpharmatics, Inc., Kirkland, WA 98034*

<sup>3</sup>*Department of Theoretical and Applied Mechanics, Cornell University, Ithaca, NY 14853*

**Abstract.** Heat generation in metals during high-strain-rate plastic deformation was investigated. Experiments were designed to measure the partition of plastic work into heat and stored energy during dynamic deformations under adiabatic conditions. A Kolsky pressure bar was used to determine mechanical properties at high strain rates while a servo-hydraulic material testing system was used at low strain rates. For dynamic loading, in-situ temperature changes were measured using a high-speed infrared detector. The dependence of the fraction of plastic work converted to heat on strain and strain rate was determined for an aluminum 2024-T3 alloy and  $\alpha$ -titanium. The flow stress and the fraction of plastic work converted to heat for 2024-T3 aluminum alloy were found to be a function of strain but not of the strain rate while they were found to be strongly dependent on strain rate for  $\alpha$ -titanium.

### INTRODUCTION

When metals deform plastically, significant amounts of heat can be generated, especially in cases of highly localized deformation. If the deformation process is rapid, heat generation can lead to large temperature increases since there is no time to conduct heat away from the deforming metal, conditions become essentially adiabatic. The temperature increase can cause thermal softening in the metal and alter its mechanical performance. Even at moderate strain rates, plastic deformation can often be treated as essentially adiabatic. Understanding the coupling between plastic deformation and heat evolution is fundamental to predicting temperature fields, and associated thermal softening, in processes involving high-strain-rate deformation. Examples of applications where accurate models for heat generation are necessary include high-speed machining, ballistic penetration, shear banding, dynamic void collapse and growth, and dynamic fracture.<sup>[1-5]</sup>

Part of the mechanical energy expended during a plastic deformation process in metals is converted into heat, while the remainder stored in the material microstructure. The stored energy is an essential feature of the cold-worked state, and represents the change in internal energy of the metal. In addition the stored energy of cold work remains in the material after removal of external loads. It is generally accepted that most of the mechanical energy is dissipated as heat during plastic deformation. The fraction of the rate of plastic work dissipated as heat  $\beta$  is often assumed to be a constant parameter of 0.9, for most metals. Measurements of the ratio of stored energy to dissipated energy have varied considerably, even for nominally similar materials. Here we present an experimental methodology for measuring  $\beta$  at different plastic strains and strain rates. The experimental results clearly show that  $\beta$  could indeed be a function of these variables. The theoretical thermodynamical foundations leading to the observed plastic strain and strain rate

dependence of  $\beta$  have been discussed by Rosakis *et al.*<sup>[6]</sup>

For elasto-plastic solids, a number of assumptions are often made, including infinitesimal deformations, the additive decomposition of strain into elastic and plastic parts, a relation between stress and elastic strain identical to that of isotropic linear thermoelasticity, and linear Fourier heat conduction law. These reduce the first law, or energy balance equation, to the following customary form under conditions of uniaxial stress,

$$\rho c \dot{\theta} - k \theta_{xx} = \beta \sigma \dot{\epsilon}^P - \alpha E \theta \dot{\epsilon}^e. \quad (1)$$

Here  $\theta$  is absolute temperature,  $\sigma$ ,  $\epsilon^e$  and  $\epsilon^P$  are the components of stress, elastic strain and plastic strain, respectively, viewed as functions of coordinate  $x$  and time  $t$ ; subscripts indicate partial derivatives with respect to the corresponding variable and superposed dots denote time derivatives. The material constants  $\rho$ ,  $c$ ,  $k$ ,  $\alpha$ ,  $E$ ,  $\nu$  are mass density, specific heat, thermal conductivity, thermal expansion coefficient, Young's modulus and Poisson's ratio, respectively.

It is assumed that some of the irreversible plastic work contributes to heat generation, while the rest is stored as energy of crystal defects accompanying plastic deformation, traditionally known as the *stored energy of cold work*. Hence  $\beta$  in (1) is the *fraction of plastic work rate*  $\dot{W}^P = \sigma \dot{\epsilon}^P$  converted into *thermoplastic heating*  $\dot{Q}^P = \beta \sigma \dot{\epsilon}^P$ , i.e.,  $\beta = \dot{Q}^P / \dot{W}^P$ . Unfortunately, there seems to be no consensus on quantitative aspects of the stored energy of cold work. If adiabatic conditions prevail and the thermoelastic heating  $\dot{Q}^e = -\alpha E \theta \dot{\epsilon}^e$  is negligible compared to the thermoplastic heating, (1) simplifies to  $\rho c \dot{\theta} = \beta \sigma \dot{\epsilon}^P$ , allowing one to write

$$\beta = \frac{\rho c \dot{\theta}}{\sigma \dot{\epsilon}^P}. \quad (2)$$

As a result, under adiabatic conditions,  $\beta$  can be measured from experimental records of the temperature, stress and plastic strain versus time.

G. I. Taylor first published a series of papers on the latent energy remaining in metals after cold working.<sup>[7,8]</sup> Without knowledge of microstructural mechanisms for energy storage and strain hardening, Taylor concluded that "the fact that the absorption of latent energy and the increase in strength with increasing strain both cease when the same amount of cold work has been applied suggests that the strength of pure metals may depend only on the amount of cold work which is latent in them." The review article by Bever *et al.*<sup>[9]</sup> gives a comprehensive overview of various attempts to measure the stored energy of cold work. It also covers basic thermodynamic aspects of plasticity and microstructural characteristics of the cold-worked state. Mason *et al.*<sup>[10]</sup> made the first systematic attempt to measure the strain dependence of the partition of plastic work during *dynamic* deformations.

## EXPERIMENTAL

The techniques for measuring the stored energy of cold work can be separated into two broad categories: (a) *In-situ* methods, where measurements are made during deformation, and (b) post-mortem methods, where the stored energy is measured after deformation. Detailed description of these methods can be found in the article by Bever *et al.*<sup>[9]</sup>

Typically, the amount of energy given off as heat is measured independently of the total amount of external work. The total external work is generally calculated from load-displacement data. Thus, the loading device must have the means to record all relevant forces and displacements acting on the specimen.

The Kolsky (split-Hopkinson) pressure bar<sup>[11,12]</sup> is by now a well-established apparatus for the high-strain-rate testing of metals and is shown in Fig. 1. Many references regarding this classic technique exist,<sup>[12]</sup> thus only a cursory review of the governing equations are given here. The apparatus consists of a striker bar, an input bar, and an output bar, all of which are assumed to remain elastic during a test. A specimen of length  $l$  is placed between the input and output bars. For a sample assumed to undergo homogeneous deformation, Kolsky<sup>[11]</sup> showed

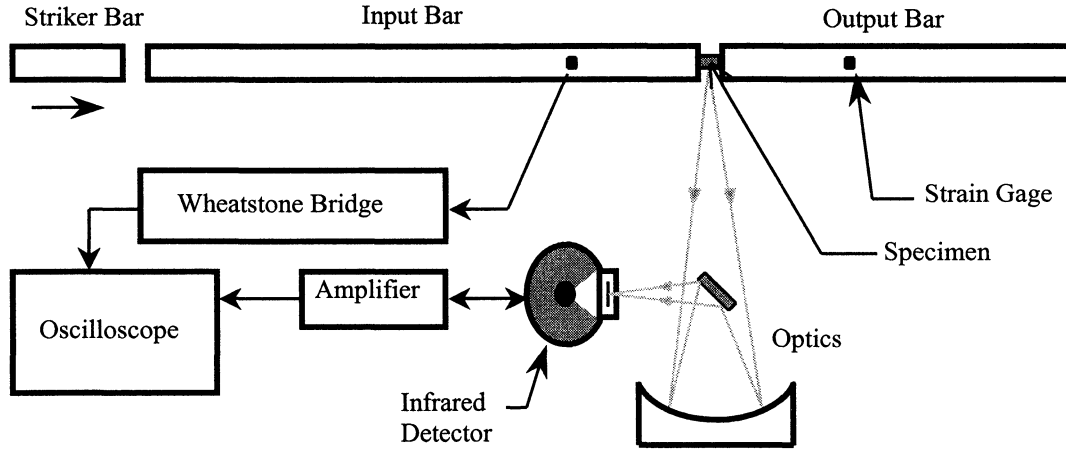


Figure 1. Schematic of Kolsky (split Hopkinson) pressure bar with high-speed infrared thermography.

that the nominal strain rate,  $\dot{\epsilon}(t)$ , is given by

$$\dot{\epsilon}(t) = -\frac{2c_0}{l} \epsilon_R(t) \quad (3)$$

where  $\epsilon_R(t)$  is the time-resolved strain of the reflected signal in the input bar and  $c_0$  is the one-dimensional bar wave speed. The strain in the sample can be calculated from (3) by integration.

The nominal stress,  $\sigma(t)$ , is calculated from the load in the output bar divided by the original sample area

$$\sigma(t) = \frac{A_0}{A} E \epsilon_T(t) \quad (4)$$

where  $A$  is the undeformed area of the specimen,  $E$  is the Young's modulus of the bar material and  $\epsilon_T(t)$  is the time-resolved strain in the output bar of cross-sectional area  $A_0$ . The input and output bars are assumed to be composed of the same material, and of identical and uniform cross-sectional area.

There exist several types of transducers available for the measurement of temperature, each having relative advantages and disadvantages. Photon detectors measure temperature remotely, have high-speed response, and thus are particularly suitable

for short time events. A single, photoconductive HgCdTe detector, with maximal responsivity of 8-12  $\mu\text{m}$ , was used for measuring temperature at high strain rates. This wavelength range was chosen to match the peak spectral power distribution of a body between 300-400 K, the range of temperatures expected during high-strain-rate deformation in a Kolsky pressure bar. The detector-amplifier combination used in the present study had a bandwidth of 5 Hz to 2MHz. DC signals were blocked by an AC-coupling capacitor located in the preamplifier circuit, thus only dynamic temperature changes could be resolved by the infrared detector.

Most IR optical systems are a variation of one of the basic catoptric telescope designs. The Newtonian system, consisting of a concave and a flat mirror, allows for easy adjustment of magnification, and formed the basis of the optical system used in the present study, see Fig. 1.

Perhaps the most important experimental issue was the calibration of the infrared detectors. For all tests included here, an experimental approach to calibration was adopted. The calibration specimen heated in a furnace to raise its temperature above the expected maximum temperature of an actual test, and placed in a holding fixture. As the specimen cooled, detector output and temperature were recorded.

To obtain large plastic strains in compression, a technique of reloading samples was used. The

reflection of input stress waves from the free end of the input bar can cause repeated loading of the sample. To avoid repeated loading during one test, a short output bar was used.<sup>[13]</sup> In this configuration, the tensile stress wave that results from reflection from the free end of the output bar will cause the output bar to pull away from the sample, ending the test before a second loading. For a given sample, the dimensions before and after testing were recorded. The sample was then remachined, resulting in a virgin surface finish. The remachined sample was then tested with a known initial value of plastic strain. This process was repeated until the desired value of plastic strain was attained.

## RESULTS

### Aluminum 2024-T3 Alloy

The engineering compressive stress versus strain curves for the aluminum 2024-T3 alloy are shown in Fig. 2 for two strain rates,  $10^{-3} \text{ s}^{-1}$  and  $3000 \text{ s}^{-1}$ . In this range of strain rates, the material behavior is found to be rate insensitive. The fraction  $\beta$  of plastic work rate converted to heating computed

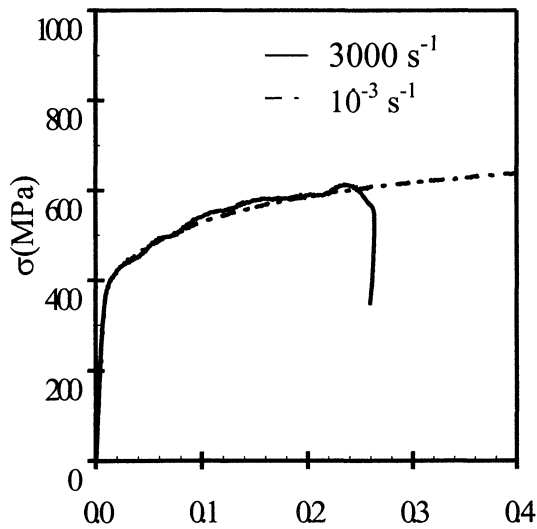


**Figure 2.** Engineering stress versus engineering strain curves at two different strain rates ( $10^{-3} \text{ s}^{-1}$  and  $3000 \text{ s}^{-1}$ ) for 2024-T3 aluminum alloy.

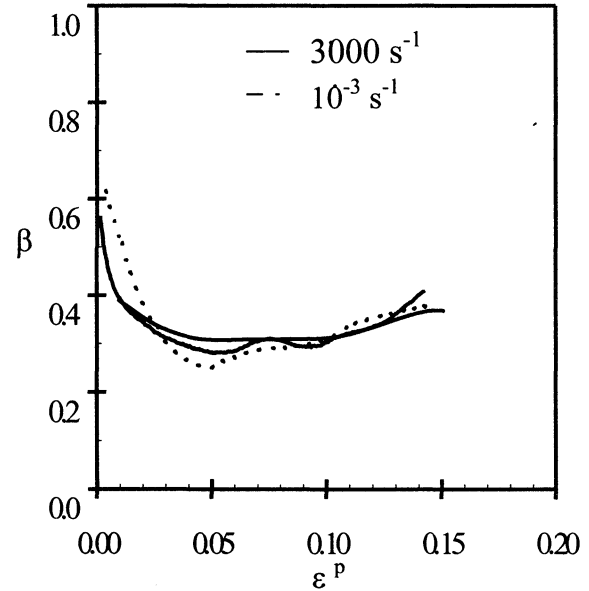


**Figure 3.** Fraction of plastic work rate converted to heating  $\beta$  vs. engineering plastic strain at two different strain rates ( $1 \text{ s}^{-1}$  and  $3000 \text{ s}^{-1}$ ) for 2024-T3 aluminum alloy.

using (2) is shown in Fig. 3 for two strain rates,  $1 \text{ s}^{-1}$  and  $3000 \text{ s}^{-1}$ . These curves represent the functional dependence of  $\beta$  on engineering plastic strain after yield for values of the latter less than 15%. The two curves at  $3000 \text{ s}^{-1}$  represent two separate tests at that strain rate, and illustrates a measure of repeatability of the experimental method. There was no observed dependence of  $\beta$  on strain rate. For plastic strains between 0.05 and 0.15, only 30-35% of plastic work was dissipated as heat.

To determine the relative partition of plastic work at higher levels of strain in compression, the reloading technique, described earlier, was employed. The calculated  $\beta$  for the large strain compression tests is shown in Fig. 4. From 0 to 0.15 plastic strain, the dependence of  $\beta$  on strain resembled that in the tests of Fig. 3. Above 0.15 plastic strain, the ability to store energy decreases and  $\beta$  rapidly increases towards 1. Above 0.4 plastic strain, nearly all input work was dissipated as heat.

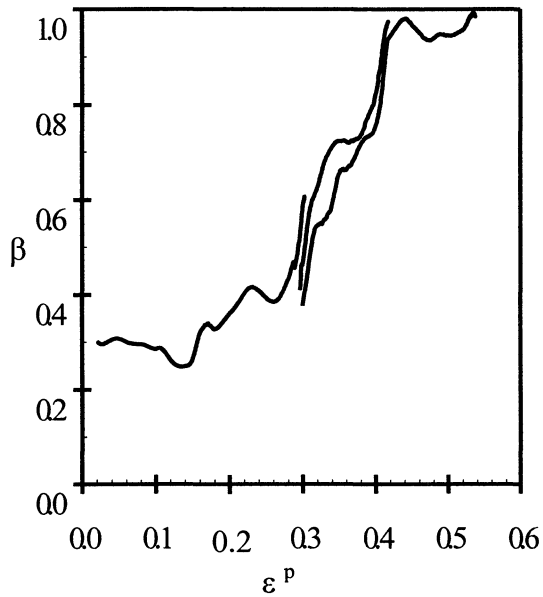


**Figure 4.** Fraction of plastic work rate converted to heating  $\beta$  vs. engineering plastic strain from successive loading sequences at and  $3000 \text{ s}^{-1}$  for aluminum 2024-T3 alloy.

#### $\alpha$ -Titanium

The true compressive stress versus true strain curves for the  $\alpha$ -titanium are shown in Fig. 5 for two strain rates,  $1 \text{ s}^{-1}$  and  $3000 \text{ s}^{-1}$ . This figure shows that the flow stress for  $\alpha$ -titanium is clearly dependent on the strain rate during loading. Large strain deformations were attained on the compression Kolsky bar by a recovery and reloading technique similar to that used for the aluminum. For  $\alpha$ -titanium and other rate-sensitive metals, extreme care must be exercised to match strain rates between loading sequences.<sup>[13]</sup>

The partition of plastic work into heat and stored energy was observed to be dependent on both strain and strain rate in  $\alpha$ -titanium. Figure 6 shows the fraction of plastic work rate converted into heating  $\beta$  plotted against engineering plastic strain during uniaxial compressive deformation. The curves shown here represent the value of  $\beta$  at low levels of

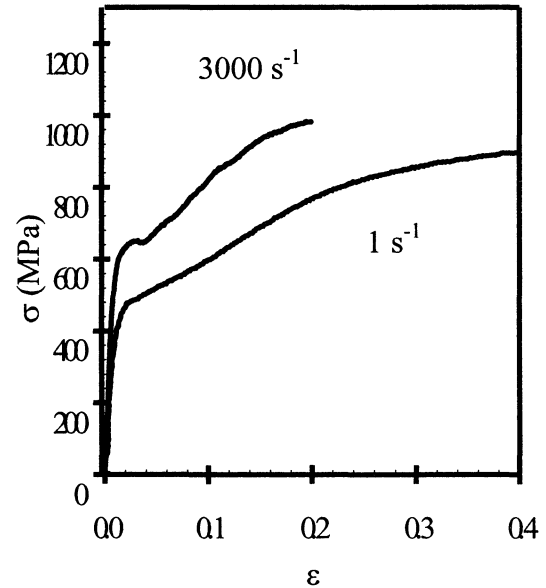


**Figure 5.** Engineering stress versus engineering strain curves at two different strain rates for  $\alpha$ -titanium.

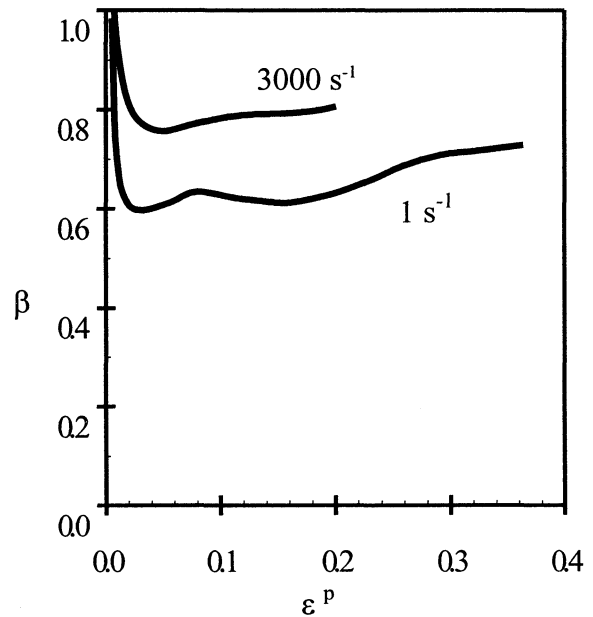


**Figure 6.** Fraction of plastic work rate converted to heating  $\beta$  vs. engineering plastic strain at two different strain rates for  $\alpha$ -titanium.

plastic strain. At a strain rate of  $1 \text{ s}^{-1}$ , titanium stored a relatively large amount of energy,  $\sim 35\%$ , just after yield. As strain increased, the ability to store energy was reduced. At higher strain rates, a smaller fraction of energy was stored at all strain levels in this range. The large strain data showed that the material cannot store energy indefinitely, and at some critical level of plastic strain nearly all of the energy was dissipated as heat, causing  $\beta$  to approach unity.<sup>[13]</sup>

Several features emerge concerning the relative amount of energy dissipation in  $\alpha$ -titanium. It is clear that  $\beta$  in titanium is a function of strain and strain rate. Near the yield point, during the stage of rapid dislocation multiplication,  $\beta$  was observed to be a rapidly decreasing function of strain at both strain rates. The relative ability of titanium to store cold work increased with decreasing strain rate. The theoretical basis for the dependence of  $\beta$  on strain rate can be found in Rosakis *et al.*<sup>[6]</sup> where the experimental results are compared with the results of a thermodynamic theoretical model.

## CONCLUSIONS

Several conclusions can be drawn regarding the conversion of plastic work into heat, as well as the experimental techniques<sup>[13]</sup> employed in the investigation:

- The adiabatic, homogenous deformation in the Kolsky (split Hopkinson) bar allowed a simple calculation of the fraction of plastic work converted into heat. The ratio of plastic work rate converted into heating  $\beta$  was treated as a variable quantity and its dependence on both strain and strain rate was investigated.
- The aluminum 2024-T3 alloy did not exhibit strain rate dependence in flow stress over the entire range of strain rates tested. At low levels of plastic strain, 2024-T3 aluminum stored more than 60% of the input plastic work. At some level of plastic strain, it could no longer store plastic work. After this point,  $\beta$  increased to a value near 1.0 and remained nearly constant during subsequent plastic deformation. The fraction of plastic work dissipated as heat was not found to be sensitive to strain rate.

- In contrast to aluminum, the flow stress of  $\alpha$ -titanium was strongly dependent on strain rate. The initial flow stress increased by more than 15% between strain rates of  $10^{-3}$  and  $3000 \text{ s}^{-1}$ . Titanium dissipated a greater proportion of energy as heat at low strains than aluminum 2024-T3 alloy. The ability to store energy in titanium decreased with increasing plastic strain. The proportion of energy dissipated as heat at fixed strain increased with strain rate. For plastic strains above 0.3, titanium dissipated nearly all input plastic work as heat.

## ACKNOWLEDGEMENTS

The research reported here was supported by the Office of Naval Research and the National Science Foundation and is gratefully acknowledged.

## REFERENCES

1. Clifton, R. J., Duffy, J., Hartley, K. A., and Shawki, T. G., *Scr. Met.* **18**, 443-448 (1985).
2. Gilman, J. J., *Mech. Mat.* **17**, 83-96 (1994).
3. Zehnder, A. T., and Rosakis, A. J., *J. Mech. Phys. Solids* **39**, 385-415 (1991).
4. Zhou, M., Ravichandran, G., and Rosakis, A. J., *J. Mech. Phys. Solids* **44**, 1007-1032 (1996).
5. Camacho, G. T., and Ortiz, M., *J. Comp. Meth. Appl. Mech. Eng.* **142**, 269-301 (1997).
6. Rosakis, P., Rosakis, A. J., Ravichandran, G., and Hodowany, J., *J. Mech. Phys. Solids* **48**, 581-607 (2000).
7. Farren, W. S., and Taylor, G. I., *Proc. Roy. Soc. London* **A107**, 422-451 (1925).
8. Taylor, G. I., and Quinney, H., *Proc. Roy. Soc. London* **A163**, 157-181 (1937).
9. Bever, M. B., Holt, D. L., and Titchener, A. L., *Prog. Mat. Sci.* **17**, 1-190 (1973).
10. Mason, J. J., Rosakis, A. J., and Ravichandran, G., *Mech. of Materials* **17**, 135-145 (1993).
11. Kolsky, H., *Proc. Roy. Soc. London* **B62**, 676-700 (1949).
12. Gray, G. T., "Classic Split-Hopkinson Pressure Bar Testing," in *ASM Handbook*, Vol. 8, ASM International, Metals Park, OH, 2000, pp. 462-476.
13. Hodowany, J., Ravichandran, G., Rosakis, A. J., and Rosakis, P., *Exp. Mech.* **40**, 113-123 (2000).